

# The effect of titanium slag on the properties of glass-ceramic composites from South African coal fly ash

AM Modiga, A Mwamba

Mintek, 200 Malibongwe Drive, Randburg, 2194, South Africa  
Email: agnesm@mintek.co.za

## Abstract

In this study, the impact of titanomagnetite slag on the structure of glass-ceramic composites was investigated. The slag was added as a source of titania which promotes nucleation within the parent glass matrix and magnesium oxide which facilitates crystallisation. A mixture of fly ash and varying quantities of waste beverage glass and titanomagnetite slag were melted. The melts were then annealed at lower temperatures to reduce the internal stress and, subsequently, cooled to room temperature to produce parent glasses. The mass of fly ash was held constant at 60%, while the mass of the waste beverage glass and titanomagnetite slag was varied between 10-30% and 0-30% respectively. Afterwards, the parent glasses were converted to glass-ceramic composites through a controlled double-staged thermal treatment. Characterisation of these composites showed that an increase in titanomagnetite slag resulted in many crystal phases forming within the glass-ceramic matrix and an increased porosity. The desired diopside phase was not detected in the composites same as when pure magnesium oxide was added instead of the titanomagnetite slag. The compressive strengths, the bulk densities and melting temperatures of the glass-ceramic composites were found to be lower as compared to glass-ceramic composites produced from a mixture containing pure magnesium oxide. However, they were highly resistant to attack by nitric acid and sodium hydroxide.

## 1. Introduction

Circular economy is now considered to provide an opportunity for sustainable economic growth. This translates to simultaneously reducing material inputs and waste outputs while continuing to generate revenue. Coal fly ash and metalliferous slags have been some of the waste streams which are challenging to discard in South Africa, due to them containing substances. Thus, there has been initiatives for their utilization, such as the production of glass-ceramic composites so as to rapidly reduce their disposal. It is however important to note that fly ashes have varying chemical compositions due to the origin of the parent coal and the furnace operation, yielding varying properties of the glass-ceramic composites. Generally, glass-ceramic composites are fine grained polycrystalline composites with excellent mechanical properties produced by controlled crystallization of the parent glasses (Rawlings et al., 2006). The excellent properties mainly depend on the content and distribution of the crystals and glass phases of glass-ceramic. The value of the glass-ceramic composites can be significantly higher than that of traditional ceramics due to their exceptional functionalities and their specialised applications (Zanoto, 2010; Rincón et al., 2016).

Due to the comprehensiveness of the process of producing glass-ceramics, a wide range of the silicate waste materials have been used (Rawlings et al., 2006). Taking the composition of raw materials into consideration, pure non-waste materials are added to enhance the properties of the glass-ceramic composites. However, the process aims at using larger quantities of the silicate wastes, while reducing the quantities of these pure materials added. Thus the silicate wastes are at times mixed to exploit their chemical composition for enhancing the properties of the final product (Rawlings et al., 2006). Previously, fly ash and beverage waste

bottles were used in the production of glass-ceramic composites whose compatibility was close to stones and granite in terms of compressive strength and the coefficient of thermal expansion (Modiga et al., 2019). Pure magnesium oxide (MgO) was added to facilitate crystallization which is key in achieving the excellent mechanical properties of the glass-ceramic composites. Beverage waste bottles served as a source of additional silica (SiO<sub>2</sub>) and basic oxides like sodium oxide (Na<sub>2</sub>O) and calcium (CaO) essential in the glass making process.

Metalliferous slags with high contents of SiO<sub>2</sub>, alumina (Al<sub>2</sub>O<sub>3</sub>) and calcium oxide (CaO) with lower amounts of MgO have been reported to be excellent raw materials for the glass-ceramic production process (Nel and Tauber, 1970; Rincón et al., 2016). In some instances, other silicate sources have been added to the metallurgical slag to increase the silica content (Zhao et al., 2012). Nucleating agents such as TiO<sub>2</sub>, chromium oxide (Cr<sub>2</sub>O<sub>3</sub>) and iron oxide (Fe<sub>2</sub>O<sub>3</sub>) have been added to facilitate bulk nucleation and crystallization, leading to excellent mechanical properties of the final product (He et al., 2017).

Addition of three nucleation agents TiO<sub>2</sub>, Cr<sub>2</sub>O<sub>3</sub> and Fe<sub>2</sub>O<sub>3</sub> to blast-furnace slags (BFS) yielded slag-based glass-ceramics with a pyroxene, diopside as the main crystalline phase (He et al., 2017). The produced glass-ceramics had a bending strength of 114.74 MPa and a bulk density of 2.77 g/cm<sup>3</sup>. When 5% TiO<sub>2</sub> was added to Turkish BFS, followed by a double staged heat treatment, gehlenite (Ca<sub>2</sub>Al<sub>2</sub>SiO<sub>7</sub>) and akermanite (Ca<sub>2</sub>MgSi<sub>2</sub>O<sub>7</sub>) phases were formed in the glass-ceramic composites (Öveçoğlu, 1998) at an optimum crystallization temperature of 1100°C. The composites had a bending strength and microhardness value of 340 MPa and 1020 kg mm<sup>-2</sup> respectively.

Wu *et al.* (2006) mentioned that glasses containing between 2 and 20 wt% TiO<sub>2</sub> crystallised with the formation of uniform fine-grained microstructures. The required maximum quantities of TiO<sub>2</sub> are reliant on the composition of the glass and are inversely proportional to the SiO<sub>2</sub> content. TiO<sub>2</sub> was effective since it induced bulk crystallization. Though amounts exceeding 20 wt% yielded the precipitation of TiO<sub>2</sub> and a decline in the nucleation and growth of the desired crystalline phases.

Taking the study by Modiga *et al.* (2019) as the basis, this paper reports on the study of the effects of MgO replacement with a silicate waste, a titanomagnetite slag and varying quantities of beverage waste glass on the microstructure and properties of the glass-ceramic composites.

## 2. Experimental

### 2.1 Preparation of materials

Fly ash from a South African power station, beverage waste bottles and a titanomagnetite slag were used as raw materials. The titanomagnetite slag was produced from the smelting of titanomagnetite ore to recover iron and vanadium in an open slag bath furnace setup. The chemical composition and mineralogical characterization of the fly ash and the waste glass were reported in the previous study (Modiga *et al.*, 2019). The chemical composition of the titanomagnetite slag was determined through inductively coupled plasma optical emission spectrometry (ICP-OES).

The mass ratios in Table 1 were used for the production of three parent glasses. Varying amounts of waste glass and slag were added in order to determine their effect on both the glass and glass-ceramic samples. The raw material was mixed and milled to increase homogeneity. The procedure in Modiga *et al.* (2019) was followed to produce the parent glasses.

**Table 1:** Quantities of raw material used

	G1	G2	G3
Fly ash (wt %)	60	60	60
Beverage waste glass (wt %)	30	20	10
Titanomagnetite slag (wt %)	10	20	30

In order to convert the parent glasses to glass-ceramic composites, a two-staged thermal treatment was employed. The thermal treatment process involved a low temperature heat treatment, to initiate nuclei growth at a reasonable rate thus forming a high density of nuclei throughout the interior of the glass, proceeded by a higher temperature heat treatment to induce crystallization. The thermal treatment procedure created by Modiga *et al.* (2019) was followed to produce the parent glasses.

### 2.2 Characterization of the titanomagnetite slag and glass-ceramic composites

The amorphous and the crystal phases in the glass-ceramic composites were identified through X-ray powder diffraction (XRD). The analysis was performed using a Bruker D8 Advance powder diffractometer, with LynxEye detector and Co-K $\alpha$  radiation from 3-80° (2 $\theta$ ) with a 0.02° step size. The phases were identified using DIFFRACplus EVA software. Phase identification was based

on the net intensity of the main peaks of the phases, and the crystal structure of phases that occurred in amounts greater than 3 mass %. The effectiveness of this technique is reliant on the diffraction behaviour of the individual phases.

Scanning Electron microscopy (SEM) was used to characterize the microstructure of the glass-ceramic composites. Energy dispersive spectrometry (EDS) analysis was performed on the glass-ceramic composites, using a Zeiss EVO-MA15 scanning electron microscope (SEM) fitted with Bruker energy dispersive spectroscopy (EDS) detector and Quantax software. The primary focus of the analysis was on determining the chemical composition of both crystalline and non-crystalline phases using EDS elemental analysis. Backscattered electron (BSE) images were taken to show the identified phases.

### 2.3 Mechanical and physical properties of the glass-ceramic composites

The mechanical and physical characteristics of the glass-ceramic composites were evaluated using methods registered with the South African National Accreditation System (SANAS). In order to quantify the percentage fraction occupied by the porosities, polished specimens of the glass-ceramic composites were analysed with a DSX510 optical microscope. Thermal expansions were carried out according to works procedure CER-WP-317 (Rev 01) to measure the effect of temperature on the size of the samples at constant pressure.

For the determination of the bulk density, the masses of the samples were taken and the volume measurements were achieved by immersing the samples in water and calculating the change in volume ( $\Delta V$ ) by using the change in height ( $\Delta h$ ) of the water. A cylindrical plastic beaker with a radius of 1.937cm was filled with 100ml of water to perform this exercise. Thereafter the density was obtained by dividing the mass by the volume of water displaced. To assess the ability of the material to resist failure under a compressive load, a static loading Instron 1175 tensile/compression machine was used. A rate of 3.0 mm per minute was selected and the program was set to stop if there was any movement or irregularities larger than 40 percent of the rate of test. To determine the chemical resistivity of the glass-ceramic composites, a method conducted by Modiga *et al.* (2019) was followed.

## 3. Results and discussions

### 3.1 The chemical composition of the raw materials

As reported in the previous study by Modiga *et al.* (2019), the fly ash was “class F” fly ash having higher quantities of SiO<sub>2</sub> which is a network former. Noticeable amounts of the oxides, CaO and MgO which modify the structure of the glass were also detected in the fly ash and as well as the oxides that act as intermediates which are Al<sub>2</sub>O<sub>3</sub>, TiO<sub>2</sub> and Fe<sub>2</sub>O<sub>3</sub>. Depending on the quantities of TiO<sub>2</sub> and Fe<sub>2</sub>O<sub>3</sub>, these two oxides also play a role of nucleants during conversion of the parent glass to glass-ceramics (Wu *et al.*, 2006; Erol *et al.*, 2007). Additionally, depending on the oxidation state of iron (Fe) in the melt, it acts as both a network former and a network modifier when it is ferric iron (Fe<sup>3+</sup>), and when it is ferrous

**Table 2:** Chemical composition of the titanomagnetite slag (wt %)

Al <sub>2</sub> O <sub>3</sub>	CaO	Cr <sub>2</sub> O <sub>3</sub>	Fe <sub>2</sub> O <sub>3</sub>	MgO	MnO	SiO <sub>2</sub>	TiO <sub>2</sub>	V <sub>2</sub> O <sub>5</sub>
15.0	16.1	0.2	7.0	12.1	0.8	18.3	29.5	1.05

**Table 3:** Main phase compositions of the glass-ceramic composites with different MgO contents

Phases (wt %)	Glass phase	Orthoclase	Pyroxene (Augite)	Dmisteinbergite	Anorthite	Sanidine	Högbomite	Hornblende	Iron phosphate	Diaspore	Indialite	Tridymite	Mullite	Spinel	Corundum
10	98	1.5	0.4	-	-	-	-	-	-	-	-	-	-	-	-
20	2	-	-	24.8	14.9	13.9	12.9	11.8	9.9	3.8	4.9	3.1	-	-	-
30	0	-	-	19.8	24.9	10.5	-	-	-	-	-	3.2	13.3	11.8	16.7

iron (Fe<sup>2+</sup>), it is mostly a network modifier (Mysen, 1983). The beverage waste glass had a high amount of SiO<sub>2</sub> at more than 70% and the modifying oxides CaO and Na<sub>2</sub>O at 11.87wt% and 12.96 wt % respectively.

The chemical composition of titanomagnetite slag is shown on Table 2. TiO<sub>2</sub> was the major component in the slag at 29.5 wt%. Oxides required to form and stabilize the glass, SiO<sub>2</sub> and Al<sub>2</sub>O<sub>3</sub> were present at 18.3 wt% and 15 wt% respectively. Significant concentrations of CaO and MgO were also detected at 16.1 wt% and 12.1 wt% respectively. These oxides modify the glass structure for the formation crystal phases and CaO increases the chemical and mechanical strength of the glass-ceramic composite (Modiga et al., 2019). Additionally, MgO promotes crystallization and enhances the thermal resistance of the glass-ceramic composites.

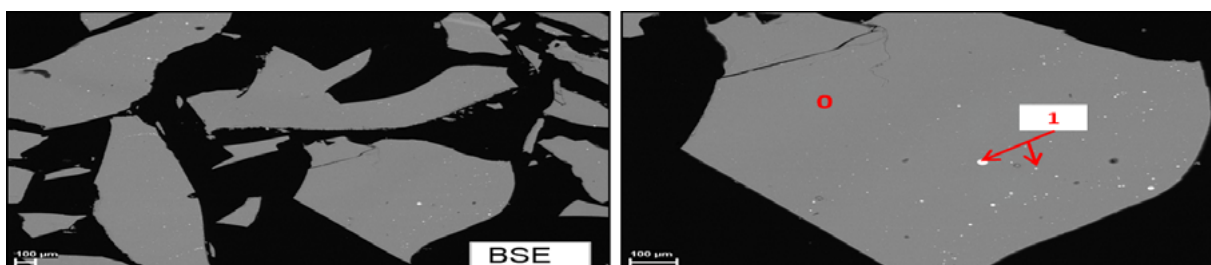
### 3.1 Characterization of glass-ceramic composites

The XRD results in Table 3 show that the glass phase of the glass ceramic composites was reduced as the slag content increased. Reduction of waste beverage glass led to the reduction of the silica content, while the concentration of the glass modifying oxides increased since they were significantly detected in both the fly ash and the slag. Consequently, non-bridging oxygens were introduced in the glass structure and the connections between the [SiO<sub>4</sub>] tetrahedrons were weakened (Modiga et al., 2019). Thus at the glass transitioning temperature, mobility of the ions was enhanced and they easily diffused from the glass matrix and ultimately rearranged to form crystal phases (Erol et al., 2007). Introduction of the titanium slag at 10 wt% resulted in the formation of crystal phases orthoclase (KAlSi<sub>3</sub>O<sub>8</sub>), which is a monoclinic potassium

feldspar at 1.5 wt% and a pyroxene phase, augite ((Ca,Na)(Mg,Fe,Al)(Al,Si)<sub>2</sub>O<sub>6</sub>) at 0.37 wt%. More than 98 wt% of the glass ceramic composite was an amorphous phase.

Increasing the titanomagnetite slag to equal proportions with the beverage waste glass resulted to a drastic decrease of the glass matrix to 2 wt% and an increase in the crystal phases formed. The orthoclase with partially ordered Si and Al ions within the tetrahedron, was transformed to another monoclinic k-feldspar, sanidine (KAlSi<sub>3</sub>O<sub>8</sub>) with its Si and Al ions disordered within the tetrahedron. New ordered feldspars of the plagioclase group composed of a metastable polymorphs of anorthite, dmisteinbergite (CaAl<sub>2</sub>Si<sub>2</sub>O<sub>8</sub>) were formed as the main phase (Zolotarev et al., 2019). Additionally, the stable anorthite (CaAl<sub>2</sub>Si<sub>2</sub>O<sub>8</sub>) and hornblende ((Ca,Na)<sub>2</sub>(Mg,Fe,Al)<sub>5</sub>(Al,Si)<sub>8</sub>O<sub>22</sub>(OH)<sub>2</sub>) were in quantities less than 15%. Minor quantities of indialite (Mg<sub>2</sub>Al<sub>4</sub>Si<sub>5</sub>O<sub>18</sub>), which is a dimorph of cordierite (Chukanov et al., 2014) were also detected as well as diaspore (AlO(OH)) and tridymite (SiO<sub>2</sub>). The titanium in the slag precipitated into Ti-magnetite, högbomite ((Mg,Fe)<sub>2</sub>(Al,Ti)<sub>5</sub>O<sub>10</sub>), which was at 12.89 wt%.

At 30% titanomagnetite slag, the glass-ceramic composites were completely crystallized with an increased formation of the plagioclase phases, anorthite in higher contents followed by dmisteinbergite. Sanidine was still present, though at slightly reduced quantities and tridymite concentration increased to 3.16 wt%. New phases mullite (3Al<sub>2</sub>O<sub>3</sub>·2SiO<sub>2</sub>) and spinel (MgAl<sub>2</sub>O<sub>4</sub>) were also detected at 13.28 and 11.77 wt% respectively. Additionally, corundum (Al<sub>2</sub>O<sub>3</sub>) was also formed at 16.67 wt%.

**Figure 1:** SEM images of the glass-ceramic composites with 10 wt% slag

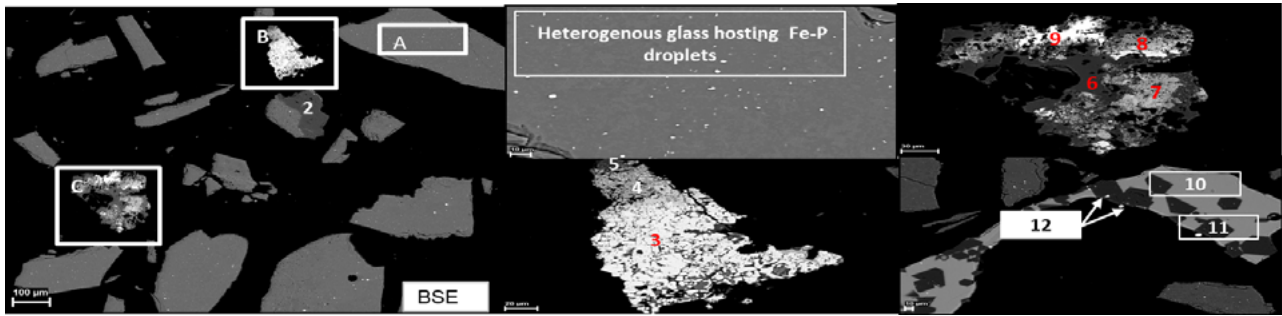


Figure 2: SEM images of the glass-ceramic composites with 20 wt% slag

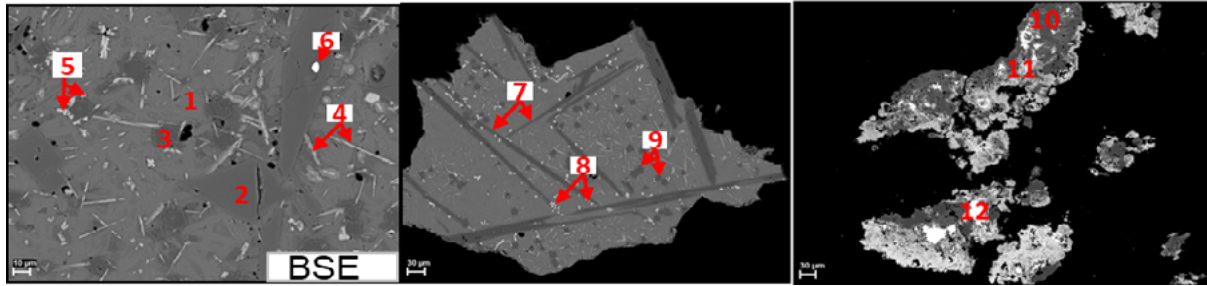


Figure 3: SEM images of the glass-ceramic composites with 30 wt% slag

SEM images of the glass-ceramic composites are showed below. In Figure 1 at 10 wt% titanium slag, the glass-ceramic composites were entirely composed of an amorphous phase at label (0) made up of light chemical elements such as Na, Al, Si, Ca, Ti and O. Isolated white blobs of FeSi at (1) were also identified on the glass phase.

Figure 2 represents the SEM images of the glass-ceramic composites with 20% slag. The plagioclase feldspar group minerals, dmisteinbergite and anorthite labelled as (10) were respectively the main and minor phases formed.

Scattered blobs of Fe-P and particles of porous and multi-phase mullite (5&6), perovskite (7), Fe-Ti oxide (8) and FeSi (9) were sporadically observed on the glass. Few cubic intergrowths of spinel (11) were also observed as well as minor particles of diaspore (2).

Figure 3, at 30 wt% slag had the plagioclase feldspar group minerals (1), anorthite and dmisteinbergite as the main phases. They were overlaid by different fully crystallised phases of mullite (10), spinel (3), needle-like structures of Ti-Al-Si oxide (4) and corundum (7).

Scattered particles of porous and multi-phased mullite (10), Ti-Fe oxide (11) and FeSi (12) were sporadically observed.

### 3.3 Physical and mechanical properties of the glass-ceramic composites

Figure 4A shows the effect of slag on the structure of the glass-ceramic composites in terms of porosity and bulk density and the predicted trends if quantities of the slag were to be increased to 50 wt%. Both parameters increased as the slag content is increased. The mineralogical analyses of the glass-ceramic composites indicated an increase in the crystal phases as the slag as increased. The density values of the glass-ceramic composites are in the ranges 1.76 – 2.65 g/cm<sup>3</sup>. The density at 2.65 g/cm<sup>3</sup> correlates with the density values of the main phases, anorthite and dmisteinbergite (~2.74-2.76 g/cm<sup>3</sup>) as indicated by Erol et al. (2007). Additionally, the porosity of the glass-ceramic composites increased as well from 9.35% to 12.15% as more crystal phases form.

The compressive strength of the glass-ceramic composites in Figure 4B increased to a maximum (71.49 MPa) at 20 wt% slag and

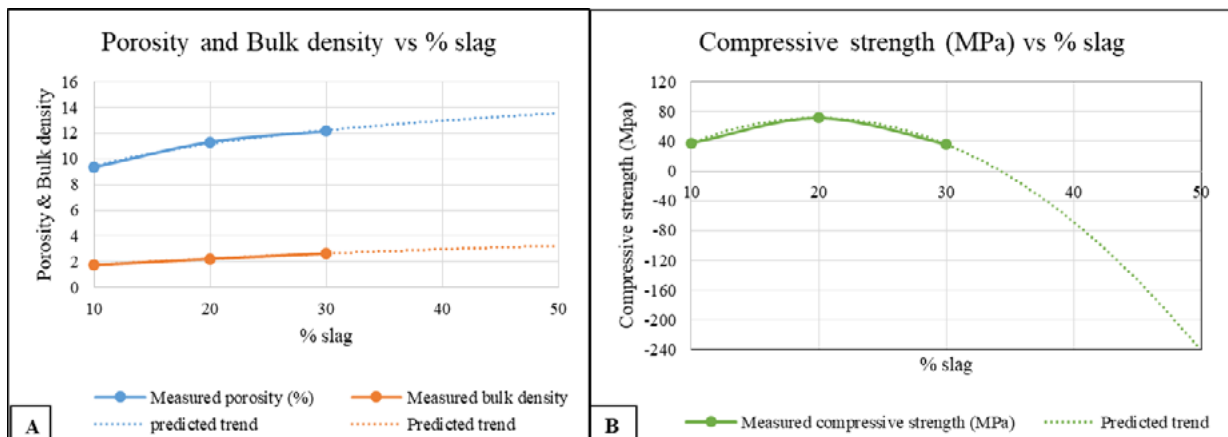


Figure 4: (A) Porosity and bulk density and (B) Vickers hardness as a function of slag content

significantly decreased afterwards to 36.07 MPa at 30 wt% slag. This can be credited to the increased crystal content and porosity in the glass-ceramic composites that promoted fracturing. The predicted trend of the graph also shows that the compressive strength will continue to decrease, which can be attributed to the amount of slag added to the mix forming more crystal phases and the increasing porosity. The Vickers hardness of the composites in Figure 5 also increased as the titanium slag content and crystallization increase. The increase was from 5.58 GPa at 10 wt% slag to 8.47 GPa at 30 wt% slag, also with the predicted increasing trend should the slag content be increased. The effect of the titanomagnetite slag on temperature resistance of the glass-ceramic composites is shown in Table 4. The coefficient of thermal expansion decreased from  $11.5 \times 10^{-6}/^{\circ}\text{C}$  to  $6.3 \times 10^{-6}/^{\circ}\text{C}$  with an increased addition of the titanomagnetite slag from 10% to 20%, though at 30% slag, it increased to  $7.0 \times 10^{-6}/^{\circ}\text{C}$ . The melting temperatures though increased indicating that the addition of slag resulted in the formation of phases that are resistant to high temperatures. Glass-ceramic composite with 30% slag had a high melting temperature.

**Table 4:** Coefficient of thermal expansion (CTE) of the glass-ceramic composites

Titanomagnetite slag wt%	Melting Temperature	CTE( $^{\circ}\text{C}$ )
10	230 $^{\circ}\text{C}$	$11.5 \times 10^{-6}$
20	750 $^{\circ}\text{C}$	$6.3 \times 10^{-6}$
30	998 $^{\circ}\text{C}$	$7.0 \times 10^{-6}$

### 3.4 Chemical resistance of the glass-ceramic composites

There were no changes on the glass-ceramic composites, after they were soaked in distilled water and then air-dried. The same results were observed for glass-ceramic composites with 10 wt% and 20 wt% slag after soakage in 10%  $\text{HNO}_3$ , except for the composite with 30 wt% slag, which developed a rustic colour without any mass losses. At 10 wt% slag, the glass-ceramic composite was also not affected by the NaOH solution, though at 20 wt% and 30 wt%, the glass-ceramic composites turned grey. They also had rust accumulations, with the composite with 20 wt% being the worst.

## 4. Conclusion

In this investigation, a mixture of three wastes, coal fly ash, titanomagnetite slag and waste beverage glass was successfully converted into anorthite-based glass-ceramic composites. This was achieved by melting them to form parent glasses and subsequently submitting the parent glasses to a two-stage thermal treatment. The following conclusions could be drawn:

- Replacement of MgO with titanomagnetite slag resulted in the formation of the plagioclase phases, anorthite and dmisteinbergite.
- No diopside phase was formed.

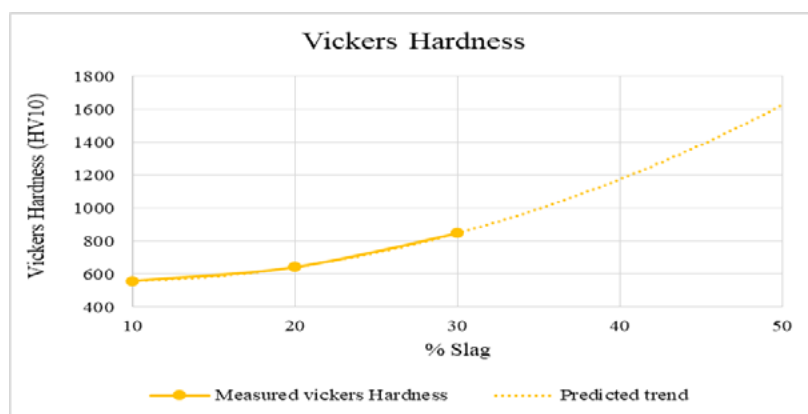


**Figure 5:** Vickers hardness as a function of slag content

- The glass-ceramic composite with 20 wt% slag displayed excellent mechanical properties.
- Increasing the slag content resulted in an introduction of modifying oxides which weakened the glass structure. Consequently, more crystal phases were formed, which had adverse effects on the mechanical properties of the glass-ceramic composites.
- The glass-ceramic composite with equal amounts of the titanomagnetite slag and waste beverage glass at 20% had a low coefficient of thermal expansion at  $6.3 \times 10^{-6}/^{\circ}\text{C}$  at 750 $^{\circ}\text{C}$ , which is lower than the ones for commercial glass-ceramic composites, Silceram and slagsital at  $7.5 \times 10^{-6}/^{\circ}\text{C}$  and  $6.5-8.5 \times 10^{-6}/^{\circ}\text{C}$  (Wu et al., 2006). It is even lower than granite and marble which are  $7 \times 10^{-6}/^{\circ}\text{C}$  each.
- The compressive stress at 20 wt% slag was 71.49 MPa, which is comparable to the ones for dolomite (50-150 MPa) and sandstone (40-200 MPa).

## Acknowledgments

The authors would like to thank Mintek for the financial and technical support as well as Cermalab for their guidance and mechanical testing of the samples.

## References

1. Chen K, Li Y, Meng X, Meng L, Guo Z. 2019. New integrated method to recover the  $\text{TiO}_2$  component and prepare glass-ceramics from molten titanium-bearing blast furnace slag. *Ceramics International*, 45(18), 24236-24243.
2. Chukanov N, Aksenov S, Pekov I, Ternes B, Schüller W, Belakovskiy D, Blass G. 2014. Ferroindialite ( $\text{Fe}^{2+}\text{Mg}$ ),  $\text{Al}_3\text{Si}_5\text{O}_{18}$ , a new beryl-group mineral from the Eifel volcanic region, Germany. *Geology of Ore Deposits*, 56(8), 637-643.
3. He D, Gao C, Pan J, Xu A. 2018. Preparation of glass-ceramics with diopside as the main crystalline phase from low and medium titanium-bearing blast furnace slag. *Ceramics International*, 44(2), 1384-1393.
4. Isa H. 2011. A review of glass-ceramics production from silicate wastes. *International Journal of Physical Sciences*, 6(30), 6781-6790.
5. Mysen, B. 1983. The structure of silicate melts. *Annual Review of Earth and Planetary Sciences*, 11(1), 75-97.
6. Modiga A, Sosibo N, Singh N. 2019. Preparation and characterization of glass-ceramic composites from South African coal fly ash. *IOP Conference Series: Materials Science and Engineering*, 655, 012038.
7. Nel P, Tauber A. 1970. Use of South African blast-furnace slag for ceramic purposes. *Journal of the South African Institute of Mining And Metallurgy*, 367.
8. Rawlings RD, Wu JP, Boccaccini AR. 2006. Glass-ceramics: their production from wastes-a review. *Journal of materials science*, 41(3), 733-761.
9. Rincón A, Marangoni M, Cetin S, Bernardo E. 2016. Recycling of inorganic waste in monolithic and cellular glass-based materials for structural and functional applications. *Journal of Chemical Technology & Biotechnology*, 91(7), 1946-1961.

10. Wu J, Rawlings R, Boccaccini A, Dlouhy I, Chlup Z. 2006. A Glass–Ceramic Derived from High TiO<sub>2</sub>-Containing Slag: Microstructural Development and Mechanical Behavior. *Journal of the American Ceramic Society*, 89(8), 2426-2433.
11. Zanotto, ED. 2010. Bright future for glass-ceramics. *American Ceramics Society Bulletin*, 89(8), 19-27.
12. Zhang W, He F, Xie J, Liu X, Fang D, Yang H, Luo Z. 2018. Crystallization mechanism and properties of glass-ceramics from modified molten blast furnace slag. *Journal of Non-Crystalline Solids*, 502, 164-171.
13. Zhao Y, Chen D, Bi Y, Long M. 2012. Preparation of low cost glass–ceramics from molten blast furnace slag. *Ceramics International*, 38(3), 2495-2500.
14. Zolotarev A, Krivovichev S, Panikorovskii T, Gurzhiy V, Bocharov V, Rassomakhin M. 2019. Dmisteinbergite, CaAl<sub>2</sub>Si<sub>2</sub>O<sub>8</sub>, a metastable polymorph of anorthite: crystal-structure and Raman spectroscopic study of the holotype specimen. *Minerals*, 9(10), 570.